PHYSICAL REVIEW C VOLUME 1, NUMBER APRIL 1970

Isobaric Analog Resonances in Proton Elastic Scattering from ^{110}Cd, ^{112}Cd, and ^{114}Cd†

V. D. Mistry,* C. L. Hollas, H. R. Hiddleston, and P. J. Riley
University of Texas, Austin, Texas 78712

(Received 8 December 1969)

Excitation functions have been measured for elastic and inelastic scattering of protons from ^{110}Cd, ^{112}Cd, and ^{114}Cd at proton energies from 6.0 to 11.0 MeV. The isobaric-analog resonances observed in ^{111}In, ^{113}In, and ^{115}In nuclei were analyzed by fitting the elastic excitation functions using a shell-model approach to reaction theory to extract quantitative nuclear-structure information for the parent analog states in ^{111}Cd, ^{113}Cd, and ^{115}Cd. Spectroscopic factors have been evaluated, and their dependence on the choice of optical and bound-state potentials has been studied. Coulomb displacement energies were also obtained from these data. Comparisons have been made with existing (d, p) work on ^{110}Cd, ^{112}Cd, and ^{114}Cd. In general, there is reasonable agreement between the (p, p_0) and (d, p) spectroscopic factors, excitation energies, orbital angular momenta, and total angular momenta.

I. INTRODUCTION

EXTENSIVE analyses of proton elastic scattering of isobaric-analog resonances have been carried out for nuclei near the closed neutron shells $N=82$ [1] and $N=126$ [2] using the theory of Weidenmüller and Mahaux.[3] A study of the centroids of the observed analog levels in the compound nucleus gives information concerning the order in which neutron shells are filled. A deviation from the simple shell-model predictions concerning the order of the nuclear levels can provide useful information on the pairing energy between two nucleons.

We have studied isobaric-analog states observed in the (p, p_0) reaction with targets of ^{110}Cd, ^{112}Cd, and ^{114}Cd. Previous ^{114}Cd(p, p_0) measurements have been reported by Hamburger *et al.*[4] Since the cadmium nuclei do not have a closed-shell structure, there is a rather large fractionization of the single-particle states. One of the aims of the present work is to use the existing experimental techniques and theoretical analyses to extract quantitative nuclear-structure information on the parent analog states in ^{111}Cd, ^{113}Cd, and ^{115}Cd from the measurement of isobaric-analog resonances in the compound nuclei ^{111}In, ^{113}In, and ^{115}In. Comparison of the spectroscopic information thus obtained with existing (d, p) work on the same targets is of interest.

Rather low-resolution (30 keV) (d, p) work on ^{110}Cd[5] and high-resolution (12 and 8 keV, respectively) (d, p) work on ^{112}Cd [6] and ^{114}Cd [7] have been carried out. The elastic (p, p) measurements do not have as high a resolution as the corresponding (d, p) work on ^{112}Cd and ^{114}Cd, but they should allow the resolution of all states observed in the existing ^{110}Cd data.

II. EXPERIMENTAL PROCEDURE

Self-supporting targets were prepared from the evaporation of isotopically enriched cadmium metal. The isotopic enrichments were as follows: ^{110}Cd, 96.6%; ^{112}Cd, 98.5%; ^{114}Cd, 99.09%. The targets were prepared by evaporating cadmium pellets made from compressed cadmium powder in a tantalum boat. Because molten cadmium does not adhere to tantalum, a copper foil was used as an adherent for the cadmium metal in the tantalum boat. To prevent the copper base from evaporating, the temperature of the boat was kept only slightly above the boiling point of cadmium.

Target thicknesses were determined from the scattering of 3.6-MeV protons. At this energy, the scattering was assumed to be purely Rutherford. The target thicknesses were 108 μg/cm^2 for ^{110}Cd, 283 μg/cm^2 for ^{112}Cd, and 305 μg/cm^2 for ^{114}Cd.

The incident proton beam for the experiments was obtained from the University of Texas EN tandem Van de Graaff accelerator. The beam energy was calibrated using the ^{27}Al(p, n) threshold and is believed to have an uncertainty of ± 20 keV. Four lithium-drifted silicon detectors were used at laboratory angles of 90°, 120°, 150°, and 170° and were cooled to dry-ice temperature to reduce noise and to improve resolution. The data consist of excitation functions for elastic scattering for c.m. proton energies between approximately 6 and 11 MeV and are shown in Figs. 1–3. For ^{110}Cd and ^{112}Cd, the energy steps between each data point were about 9 keV; for ^{114}Cd, the energy steps were approximately 18 keV. Each datum point represents from 10^4 to 10^5 counts. The relative experimental errors are caused by

---

† Research sponsored in part by the U.S. Atomic Energy Commission.

* Present address: Department of Physics, Texas Christian University, Fort Worth, Tex. 76129.

[1] S. Darmodjo, Ph.D. dissertation, The University of Texas, Austin, 1968 (unpublished); P. A. Moore, P. J. Riley, C. M. Jones, M. D. Mancusi, and J. L. Foster, Phys. Rev. **180**, 1213 (1969); G. C. Morrison, in *Nuclear Isospin*, edited by J. D. Anderson, S. D. Bloum, J. Cerry, and M. W. True (Academic Press Inc., New York, 1969), p. 435.

[2] S. A. A. Zaidi and S. Darmodjo, Phys. Rev. Letters **19**, 1446 (1967).

[3] C. Mahaux and H. A. Weidenmüller, Nucl. Phys. **89**, 33 (1966); H. A. Weidenmüller, *ibid.* **A99**, 269 (1967); **A99**, 289 (1967).

[4] E. W. Hamburger, B. L. Cohen, J. Kremenek, J. B. Moorhead, and C. Shin, Phys. Rev. **162**, 1158 (1967).

[5] B. Rosner, Phys. Rev. **136**, B664 (1964).

[6] L. H. Goldman, J. Kremenek, and S. Hinds, Phys. Rev. **179**, 1172 (1969).

[7] J. B. Moorhead, B. L. Cohen, and R. A. Moyer, Phys. Rev. **165**, 1287 (1968).

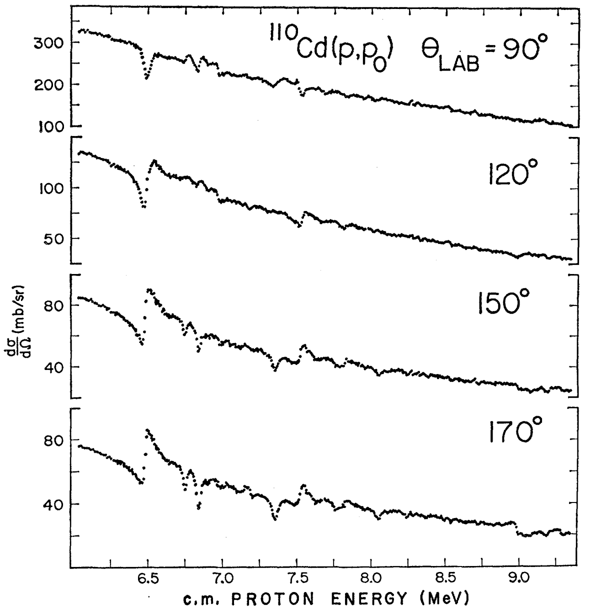

FIG. 1. Excitation functions for the elastic scattering of protons from ^{110}Cd at laboratory angles of 90°, 120°, 150°, and 170° for c.m. proton energies from approximately 6.0 to 9.4 MeV. Statistical uncertainties in the cross sections for Figs. 1–3 are smaller than the data points.

target inhomogeneity and changes in the solid angle as the beam wanders over the target. Absolute cross sections are thought to be accurate to 10%.

III. THEORETICAL ANALYSIS

The method of analysis has been described previously. Following Weidenmüller and Mahaux,[3] the energy-averaged scattering matrix for elastic scattering on spin-zero targets is given by

$$\langle S_{l_j}\rangle = \exp(2i\delta_{l_j}) - i\exp(2i\alpha_{l_j})[\Gamma_{l_j}/(E-E_R+\tfrac{1}{2}i\Gamma)], \tag{1}$$

where

$$\Gamma_{l_j} = \Gamma_{l_j}^{(A)}\left(\frac{1+2iY_{l_j}(\Delta_{l_j}/\tilde{\Gamma}_{l_j})}{1+Y_{l_j}}\right)^2 \tag{2}$$

and

$$\exp(2i\delta_{l_j}) = \exp(2i\alpha_{l_j})[(1-Y_{l_j})/(1+Y_{l_j})]. \tag{3}$$

δ_{l_j} is the optical-model phase shift for the pC system, and α_{l_j} is its real part. Δ_{l_j} is the energy shift due to the decay of a proton from an isobaric-analog resonance. All other quantities are defined in Ref. 3.

Code JULIUS[8] was used to generate theoretical elastic-scattering excitation functions using expressions (1), (2), and (3) for the scattering matrix. The code uses a potential with a surface-peaked imaginary part and a real spin-orbit part.

$$\begin{aligned} V(r) = {} & -Vf(r,r_{0r},a_r) - i4a_iW_D(d/dr)f(r,r_{0i},a_i) && \text{central}\\ & +\boldsymbol{\sigma}\cdot\mathbf{l}V_{\text{so}}(\hbar/m_\pi c)^2 r^{-1}(d/dr)f(r,r_{\text{so}},a_s) && \text{spin-orbit}\\ & +(Ze^2/2r_c)(3-r^2/r_c^2) \qquad \text{if } r\le r_c &&\\ & +Ze^2/r \qquad \text{if } r>r_c && \text{Coulomb.} \end{aligned}$$

The function $f(r,r_0,a)$ is the usual Saxon-Woods shape:

$$f(r,r_0,a)=\{1+\exp[-(r-r_0A^{1/3})/a]\}^{-1}.$$

Zaidi and Darmodjo[2] showed that the theoretical proton partial width of an analog resonance can be calculated from the expression

$$\Gamma_{l_j}(\text{th}) = (kT_0/E)\mid\langle\Phi_{nA}\mid V_1\mid\chi_{pC}^{(+)}\rangle\mid^2.$$

The radial wave functions Φ_{nA} and $\chi_{pC}^{(+)}$ are obtained by numerical integration of the homogeneous part of the Lane equations. The potentials binding the parent analog states, used in the calculation of Φ_{nA}, and the real part of the proton optical-model potential for the pC system, used in the calculation of $\chi_{pC}^{(+)}$, are related through the equation

$$T_0V_1(r)+V_p(r)=V_n(r),$$

where

$$T_0V_1/2=26(N-Z)/A,$$

in agreement with the value obtained from analysis of charge-exchange (p,n) reactions.[9] A real volume-type charge-exchange potential $V_1(r)=V_1f(r,r_0,a)$ was used. The spectroscopic factor of the analog state is then given by

$$S_{pp}=\Gamma_{l_j}^{(A)}/\Gamma_{l_j}(\text{th}).$$

Code GPMAIN,[8] a modified version of the bound-state code NEPTUNE[10] by Tamura, was used for the evaluation of theoretical proton partial widths, $\Gamma_{l_j}(\text{th})$. Code

TABLE I. Proton optical parameters used in fitting the elastic-scattering data.

	^{110}Cd(p,p_0)	^{112}Cd(p,p_0)	^{114}Cd(p,p_0)
V (MeV)	53.0	57.0	$63.0-0.20E_p$
W_D (MeV)	9.0	9.2	6.5
V_{so} (MeV)	4.0	4.0	4.0
r_{0r} (F)	1.22	1.23	1.22
r_{0i} (F)	1.22	1.22	1.22
r_{so} (F)	1.22	1.23	1.22
a_r (F)	0.63	0.64	0.63
a_i (F)	0.63	0.68	0.63
a_{so} (F)	0.63	0.66	0.63

---

[8] S. A. A. Zaidi (private communication).

[9] G. R. Satchler, R. M. Drisko, and R. H. Bassel, Phys. Rev. **136**, B637 (1964).

[10] T. Tamura, Comp. Phys. Com. (to be published).

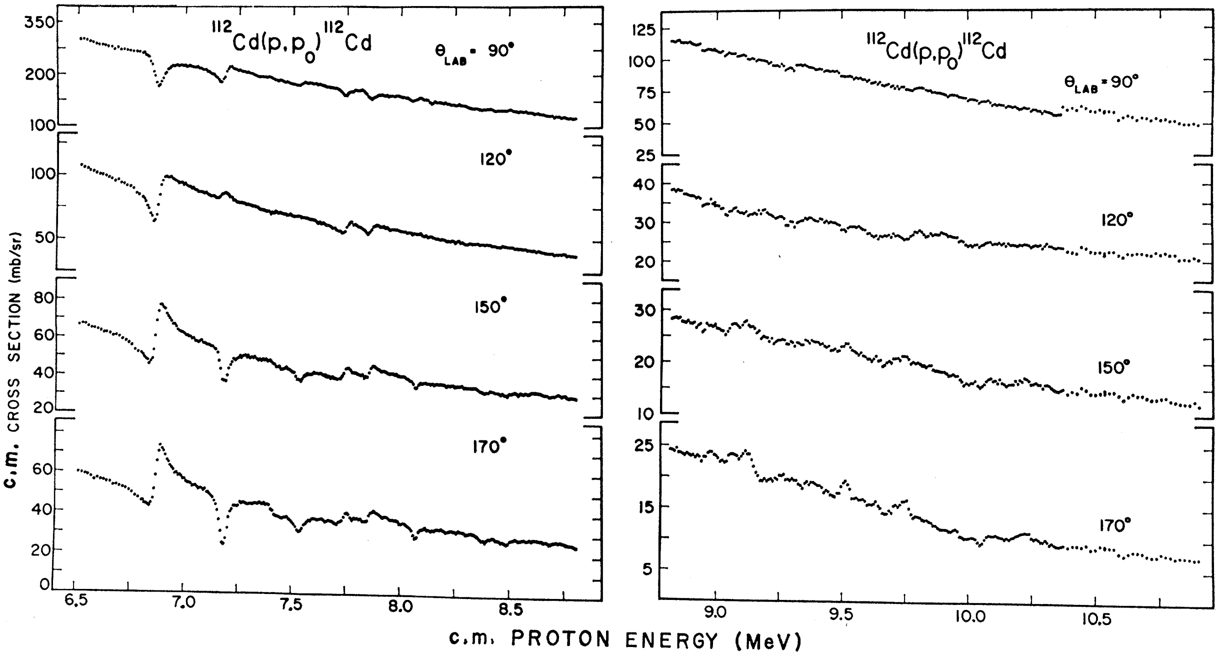

FIG. 2. Excitation functions for the elastic scattering of protons from ^{112}Cd at laboratory angles of 90°, 120°, 150°, and 170° for c.m. proton energies from 6.5 to 10.9 MeV.

GPMAIN uses the same potential as code JULIUS, except that only the spin-orbit and real central terms are employed, and no imaginary well is used.

In the analysis of $^{208}\mathrm{Pb}(p, p)$ elastic-scattering data,[2] an optical potential V_n was found that reproduced the binding energies of the $g_{9/2}$, $s_{1/2}$, $g_{7/2}$, and $d_{3/2}$ parent analog states in ^{209}Pb. The depth and geometry of the real part of the proton potential used in the scattering matrix were fixed, therefore, in accordance with the neutron potential and symmetry term. The imaginary optical parameters were then adjusted to fit the background scattering.

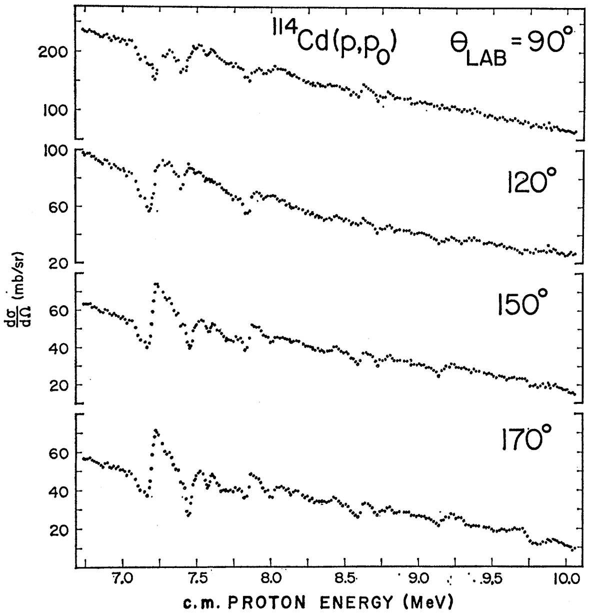

FIG. 3. Excitation functions for the elastic scattering of protons from ^{114}Cd at laboratory angles of 90°, 120°, 150°, and 170° for c.m. proton energies from 6.75 to 10.1 MeV.

Unlike ^{208}Pb, which is a doubly magic nucleus, ^{110}Cd, ^{112}Cd, and ^{114}Cd have neither neutron nor proton magic numbers. Consequently, these nuclei have rather complex shell structure. As a result, there is rather large fractionization of the various observed single-particle levels in the odd cadmium isotopes, so that it was not possible to determine exactly the binding energies of the single-particle levels. Consequently, a unique potential V_{nA} that could reproduce all the single-particle binding energies could not be found.

In the present analysis, the elastic-scattering excitation functions were first fitted by means of code JULIUS. The proton optical parameters were varied to fit the background scattering, and the resonance parameters, namely, the proton partial width $\Gamma_{l_j}{}^{(A)}$, total width Γ, the resonance energy E_R, and the level shift function Δ_{l_j}, were adjusted to give optimum agreement between the experimental data and the calculated excitation functions. In fitting the background, Perey's average parameters[11] were used as starting points. The proton optical parameters obtained in fitting the background are shown in Table I. An energy dependence of the real optical potential was found to improve the background fit for the $^{114}\mathrm{Cd}(p, p_0)$ data, and it was therefore used.

---

[11] F. G. Perey, Phys. Rev. **131**, 745 (1963).

TABLE II. Neutron binding energies and the resulting bound-state well depths used in the calculation of theoretical proton partial widths.

	^{111}Cd		^{113}Cd		^{115}Cd	
l_J	B.E. (MeV)	V_{nC} (MeV)	B.E. (MeV)	V_{nC} (MeV)	B.E. (MeV)	V_{nC} (MeV)
$s_{1/2}$	5.148	45.80	5.924	46.04	5.742	45.93
$d_{3/2}$	5.133	45.80	5.775	45.72	5.642	45.69
$d_{5/2}$	6.389	45.80	7.057	45.80	6.956	45.80
$f_{7/2}$	4.454	56.40	3.642	53.80	3.642	54.00
$p_{3/2}$	4.354	58.77	3.542	55.94	3.542	56.12

TABLE III. Resonance parameters and spectroscopic factors determined from the theoretical fits to the ^{110}Cd(p, p) elastic-scattering data. In this and Tables IV and V, $\Gamma_{l_j}{}^{(A)}$ is the partial proton width of the resonance, and Γ(total) is the total width. Quantities enclosed in parentheses are probable but not certain assignments. A comparison of the ^{110}Cd(p, p) and ^{110}Cd(d, p) analysis is also shown.

	^{110}Cd$(p, p_0)^{110}$Cd						^{110}Cd$(d, p)^{110}$Cd [a]		
$E_{\text{c.m.}}$ (MeV)	$E_{\text{c.m.}}-6.428$ (MeV)	l	J^π	$\Gamma_{l_j}{}^{(A)}$ (keV)	Γ(total) (keV)	S_{pp}	Excitation energy (MeV)	l	J^π
6.428	0.000	0	$\frac{1}{2}^+$	23.0	52.0	0.34	0.00	0	$\frac{1}{2}^+$
6.695	0.267	2	$\frac{5}{2}^+$	1.62	26.0	0.12	0.245	2	$\frac{5}{2}^+$
6.784	0.356	2	$\frac{3}{2}^+$	4.18	25.0	0.17	0.34	2	$\frac{3}{2}^+$
							0.40	5	$\frac{11}{2}^-$
(6.863)	(0.435)	(0)	$(\frac{1}{2}^+)$	2.30	40.0	(0.03)			
(6.961)	(0.533)	(0)	$(\frac{1}{2}^+)$	6.70	67.0	(0.09)			
(6.993)	(0.565)	(2)	$(\frac{5}{2}^+)$	0.48	29.0	(0.03)			
7.040	0.612	2	$\frac{5}{2}^+$	0.37	30.0	0.02	0.61	2	$\frac{5}{2}^+$
(7.089)	(0.661)	(0)	$(\frac{1}{2}^+)$	2.20	35.0	(0.03)			
(7.143)	(0.715)	(2)	$(\frac{5}{2}^+)$	1.40	52.0	(0.08)	0.70	(4)	$(\frac{7}{2}^+)$
7.290	0.862	2	$\frac{3}{2}^+$	7.60	50.0	0.26	0.86	2	$\frac{3}{2}^+$
7.458	1.030	0	$\frac{1}{2}^+$	12.00	50.0	0.15	1.02	0	$\frac{1}{2}^+$
7.511	1.083	2	$\frac{5}{2}^+$	0.08	8.0				
7.560	1.132	2	$\frac{5}{2}^+$	0.60	32.0	0.03	1.13	2	$\frac{5}{2}^+$
							1.19	0	$\frac{1}{2}^+$
7.744	1.316	0	$\frac{1}{2}^+$	12.40	90.0	0.02	1.33		
7.891	1.463	2	$(\frac{5}{2}^+)$	0.32	25.0	(0.01)			
7.983	1.555	2	$(\frac{3}{2}^+)$	2.60	35.0	(0.07)	1.55	2	$(\frac{3}{2}^+)$
8.059	1.631	(0)	$(\frac{1}{2}^+)$	0.36	24.0		1.66	0	$(\frac{1}{2}^+)$
8.173	1.745	2	$(\frac{3}{2}^+)$	1.60	35.0	(0.04)	1.72	2	$(\frac{3}{2}^+)$
8.219	1.791	(2)	$(\frac{5}{2}^+)$	0.20	15.0	(0.01)			
8.303	1.875	2	$(\frac{3}{2}^+)$	0.40	22.0	(0.01)	1.86	2	$(\frac{3}{2}^+)$
(8.393)	(1.965)	(2)	$(\frac{3}{2}^+)$	0.26	16.0	(0.01)	1.97	2	$(\frac{3}{2}^+)$
(8.423)	(1.995)	(2)	$(\frac{3}{2}^+)$	0.50	17.0	(0.01)	2.02	2	$(\frac{3}{2}^+)$
(8.467)	(2.039)	(2)	$(\frac{5}{2}^+)$	0.46	20.0	(0.01)			
(8.572)	(2.144)	(1)	$(\frac{3}{2}^-)$	0.56	30.0	(0.01)	2.14		
(8.654)	(2.226)	(2)	$(\frac{5}{2}^+)$	0.50	35.0	(0.02)	2.20		
(8.764)	(2.336)	(0)	$(\frac{1}{2}^+)$	1.60	35.0	(0.02)	2.28		
(8.810)	(2.382)	(2)	$(\frac{5}{2}^+)$	0.23	15.0	(0.01)			
8.906	2.478	3	$\frac{7}{2}^-$	2.00	35.0	0.08			
9.012	2.584	0	$\frac{1}{2}^+$	1.90	38.0	0.02			
9.123	2.695	0	$\frac{1}{2}^+$	2.40	30.0	0.03			
9.205	2.777	3	$\frac{7}{2}^-$	0.74	28.0	0.03			

[a] B. Rosner, Phys. Rev. **136,** **B664** (1964).

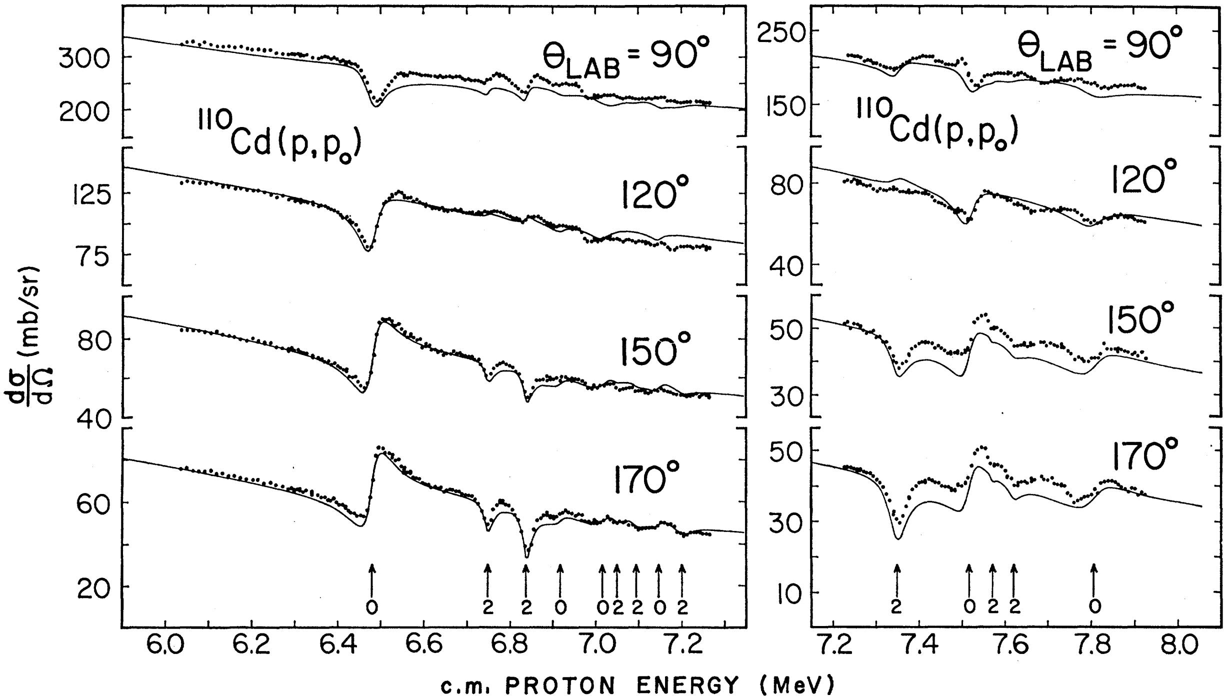

FIG. 4. Theoretical fits to the ^{110}Cd(p, p) elastic-scattering data at c.m. energies between 6.0 and 8.0 MeV. The arrows indicate the resonance energies determined from the analysis.

In order to calculate Γ_{l_j}(th), the approximate binding energies of the $s_{1/2}$, $d_{3/2}$, $d_{5/2}$, $f_{7/2}$, and $p_{3/2}$ single-particle levels in ^{111}Cd, ^{113}Cd, and ^{115}Cd, respectively, were deduced from the Cd(d, p) analyses. The bound-state well depths were then searched to give approximately these binding energies, holding the same geometry (radius and diffuseness) for the nC system as had been used for the pC system. The binding energies and the deduced well depths are tabulated in Table II. For all the three isotopes, significantly deeper well depths were obtained for the $f_{7/2}$ and $p_{3/2}$ single-particle states lying above the closed $N=82$ shell than for the s and d single-particle states below the closed shell.

The theoretical proton partial widths were then calculated using code GPMAIN. The appropriate neutron well depths, given in Table II, were used in the calculation of ϕ_{nA}. The proton real-well depth V_p, used in the calculation of χ_{pC}, was related to the neutron well depth V_n through $V_p=V_n+52(N-Z)/A$, corresponding to a symmetry term $\frac{1}{2}T_0V_1=26(N-Z)/A$ in the proton potential. Finally, the spectroscopic factors were evaluated using

$$S_{pp}=\Gamma_{l_j}{}^{(A)}/\Gamma_{l_j}(\text{th}).$$

IV. RESULTS AND DISCUSSION

For each isotope, the data clearly show a strong $l=0$ ground state followed by one or more prominant $l=2$ resonances. The resonances become progressively weaker at higher excitation energies. Above a proton energy of 9 MeV, however, clearly defined $l=3$ resonances appear in all three cases. Fits to the data were made in overlapping sections. In general, good fits were obtained; however, at the highest proton energies, where the analog resonances are weak and overlapping, good fits could not be obtained. Consequently, the resonance analyses, and particularly the spectroscopic factors, are not considered to be reliable at the highest energies. Although it is usually easy to determine the l value of an observed resonance from its shape at different angles, the shapes of the resonances are insensitive to the J values. The J-value assignments are therefore based on shell-model considerations and on previously reported (d, p) and (d, t) results.

The low-lying states with high orbital momenta $l=4$ and 5 were not observed in the elastic-scattering data because of the low penetrability of these waves to the Coulomb barrier. Further, the high resolution of the ^{112}Cd(d, p) and ^{114}Cd(d, p) work allowed the identification of more levels than could be observed in the (p, p_0) measurements. However, the identification of the $l=3$ states at rather high excitation energies appears more reliable in the (p, p_0) work than in the corresponding (d, p) measurements.

Theoretical fits to the data are shown in Figs. 4–9. The arrows on the energy axis indicate the positions of the resonances. For each resonance, the resonance parameters were kept the same for all four scattering angles. The resonance parameters obtained from the theoretical fits to the experimental data, the l and J

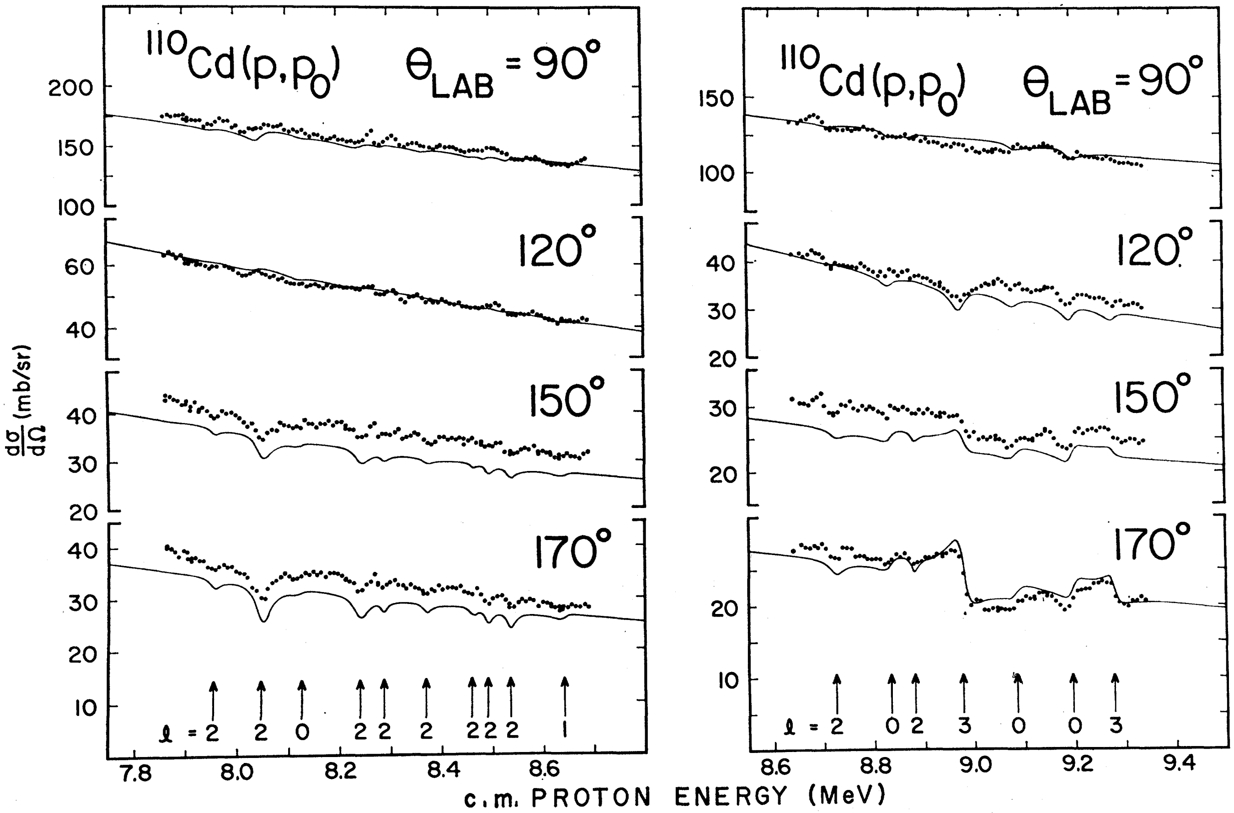

FIG. 5. Theoretical fits to the ^{110}Cd(p, p) elastic-scattering data at c.m. energies between 7.8 and 9.4 MeV. The arrows indicate the resonance energies determined from the analysis.

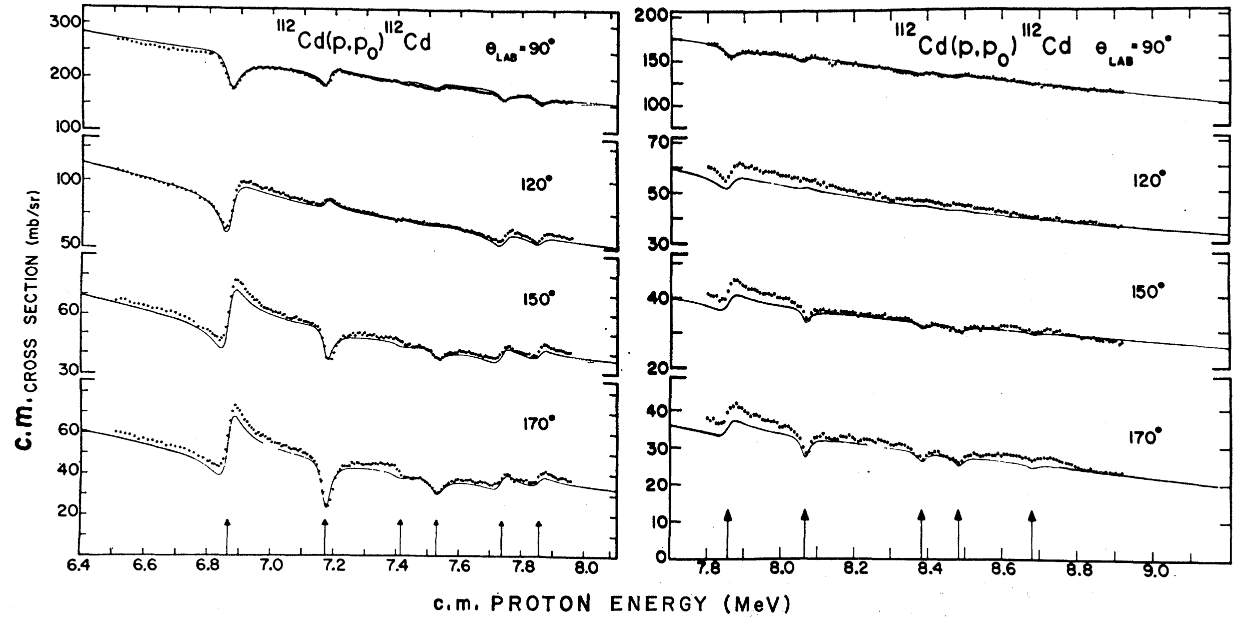

FIG. 6. Theoretical fits to the ^{112}Cd(p, p) elastic-scattering data at c.m. energies between 6.5 and 9.1 MeV. The arrows indicate the resonance energies determined from the analysis.

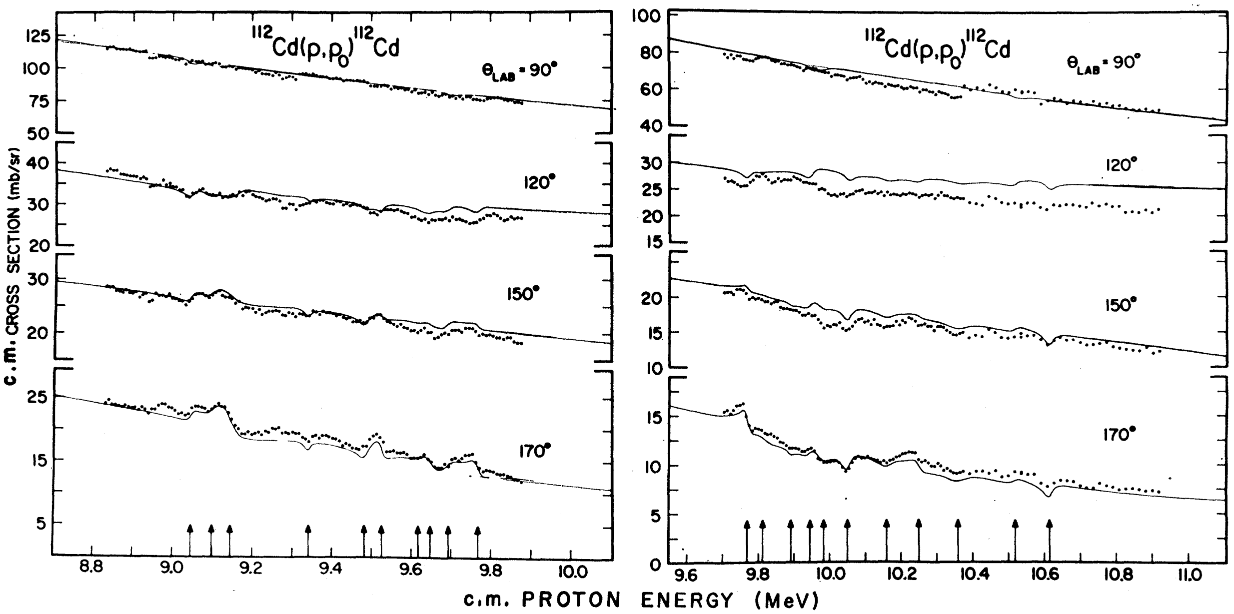

FIG. 7. Theoretical fits to the ^{112}Cd(p, p) elastic-scattering data at c.m. energies between 8.8 and 11.0 MeV. The arrows indicate the resonance energies determined from the analysis.

assignments, and the spectroscopic factors S_{pp} are given in Tables III–V. The results of the previously reported (d, p) work are also shown. Spectroscopic factors are not available for the ^{110}Cd(d, p) work. For most states, there is a one-to-one correspondence between the low-lying levels as observed in the two experiments. In nearly all cases, the spectroscopic factors S_{pp} for $s_{1/2}$ states are larger than the spectroscopic factors S_{dp} obtained for their parent states. Morrison[2] reports that S_{pp} values for low l values are in general greater than S_{dp} values and concludes that for $l=0$, this discrepancy may be due to an underestimate of S_{dp} caused by the lack of experimental data at 0°, where the maximum for the (d, p) $l=0$ angular distribution lies, and by the high sensitivity of DWBA calculations for $l=0$.

The tables are discussed in detail below. The over-all

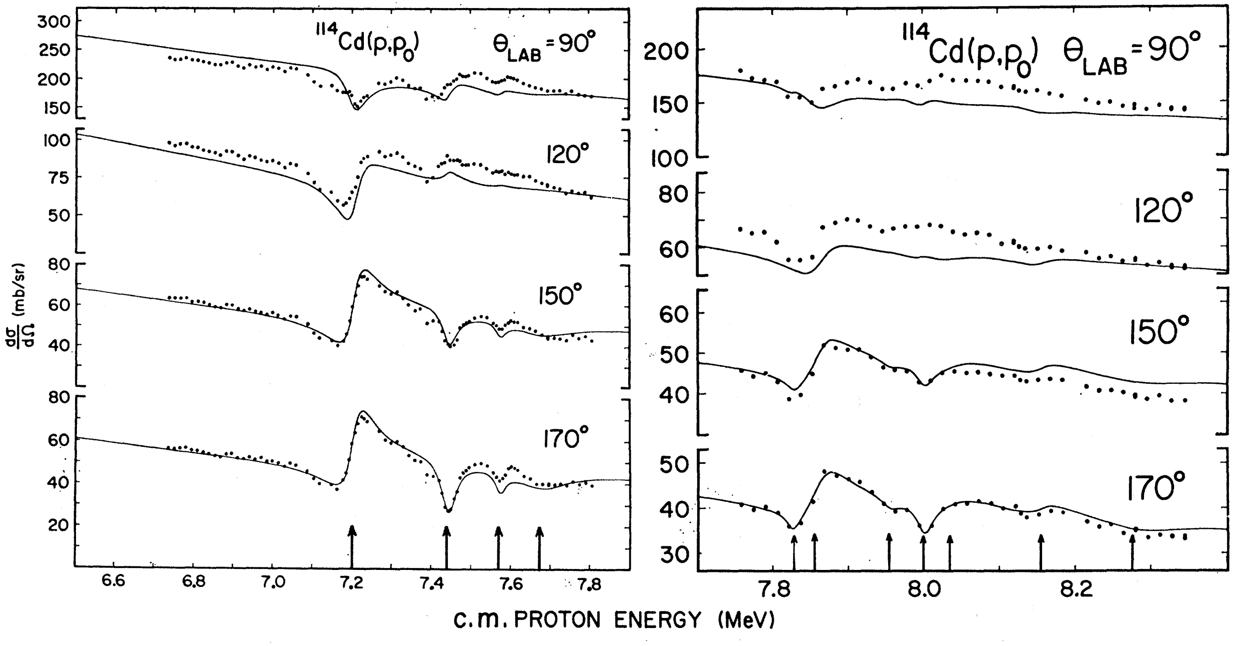

FIG. 8. Theoretical fits to the ^{114}Cd(p, p) elastic-scattering data at c.m. energies between 6.7 and 8.4 MeV. The arrows indicate the resonance energies as determined from the analysis.

TABLE IV. Resonance parameters and spectroscopic factors determined from the theoretical fits to the ^{112}Cd(p, p) elastic-scattering data. A comparison of the ^{112}Cd(p, p) and ^{112}Cd(d, p) analyses is also shown.

^{112}Cd$(p, p_0)^{112}$Cd							^{112}Cd$(d, p)^{113}$Cd^{a}			
$E_{\text{c.m.}}$ (MeV)	$E_{\text{c.m.}}-6.799$ (MeV)	l	J^{π}	$\Gamma_{lj}^{(A)}$ (keV)	Γ(total) (keV)	S_{pp}	Excitation energy (MeV)	l	J^{π}	S_{dp}
6.799	0.000	0	$\frac{1}{2}^{+}$	21.0	50.0	0.44	0.00	0	$\frac{1}{2}^{+}$	0.34
							0.27	5	$\frac{11}{2}^{-}$	0.40
7.106	0.307	2	$\frac{3}{2}^{+}$	7.2	33.7	0.38	0.30	2	$\frac{3}{2}^{+}$	0.40
							0.32	2	$\frac{5}{2}^{+}$	0.14
							0.46	4	$\frac{7}{2}^{+}$	0.26
							0.53	4	$\frac{7}{2}^{+}$	0.36
7.343	0.544	2	$\frac{3}{2}^{+}$	1.0	45.0	0.05	0.59	2	$(\frac{5}{2}^{+})$	0.05
7.457	0.658	2	$\frac{3}{2}^{+}$	3.5	47.0	0.15	0.68	2	$(\frac{3}{2}^{+})$	0.27
							0.76	0	$\frac{1}{2}^{+}$	0.14
							0.82	4	$\frac{7}{2}^{+}$	0.12
7.664	0.865	0	$\frac{1}{2}^{+}$	7.0	50.0	0.11	0.88	0	$\frac{1}{2}^{+}$	0.07
							0.90	2	$\frac{3}{2}^{+}$	0.21
							0.96			
7.783	0.984	0	$\frac{1}{2}^{+}$	4.60	50.0	0.07	0.98	0	$\frac{1}{2}^{+}$	0.04
							1.01			
							1.13±0.02			
							1.17±0.02			
7.990	1.191	2	$\frac{5}{2}^{+}$	0.96	25.0	0.04	1.20	2,3		
							1.28	2	$(\frac{5}{2}^{+})$	0.03
							1.32			
							1.39±0.02			
							1.43	2	$(\frac{3}{2}^{+})$	0.06
							1.45±0.02			
8.305	1.506	2	$\frac{3}{2}^{+}$	0.88	30.0	0.03	1.49	2	$(\frac{3}{2}^{+})$	0.06
							1.54			
							1.58	3?	$(\frac{7}{2}^{-})$?	0.02
8.404	1.605	2	$\frac{3}{2}^{+}$	0.97	31.8	0.03	1.61	2	$(\frac{5}{2}^{+})$	0.02
							1.67	(2)	$(\frac{3}{2}^{+})$	0.02
(8.599)	(1.800)	(2)	$(\frac{5}{2}^{+})$	0.26	35.0	(0.01)	1.81			
							1.84	1, 2		
							1.88			
							1.90	(0)	$(\frac{1}{2}^{+})$	0.02
							1.99			
							2.04	3	$\frac{7}{2}^{-}$	0.04
							2.08	(0)	$(\frac{1}{2}^{+})$	0.01
							2.11	3?	$\frac{7}{2}^{-}$?	0.02
							2.12±0.02			
							2.14±0.02	0??		
8.959	2.160	0	$\frac{1}{2}^{+}$	1.50	30.0	0.02	2.17	1	$\frac{3}{2}^{-}$	0.04
(9.012)	(2.213)	(0)	$(\frac{1}{2}^{+})$	1.40	40.0	(0.02)	2.18	1	$\frac{1}{2}^{-}$	0.03
9.057	2.258	3	$\frac{7}{2}^{-}$	1.73	58.0	0.06	2.24	3??		
							2.27			
							2.31	1?	$\frac{3}{2}^{-}$?	0.01
							2.33			
							2.37			
							2.41	4??		
(9.251)	(2.452)	(1)	$(\frac{3}{2}^{-})$	0.60	18.0	(0.01)	2.44			
							2.54	3?	$\frac{7}{2}^{-}$?	0.03
9.392	2.593	1	$\frac{3}{2}^{-}$	1.80	34.0	0.02	2.58	1?	$\frac{3}{2}^{-}$?	0.02
							2.63	0?	$\frac{1}{2}^{+}$?	0.04
9.434	2.635	3	$\frac{7}{2}^{-}$	0.54	25.0	0.02	2.69			
(9.526)	(2.727)	(1)	$(\frac{3}{2}^{-})$	0.30	30.0		2.75			
9.555	2.756	(3)	$(\frac{7}{2}^{-})$	0.63	38.0	(0.02)	2.77	1?	$\frac{3}{2}^{-}$?	0.02
(9.600)	(2.801)	(0)	$(\frac{1}{2}^{+})$	1.80	40.0	(0.02)	2.81	0	$\frac{1}{2}^{+}$	0.03

TABLE IV. (*Continued*).

^{112}Cd(p, p_0)^{112}Cd							^{112}Cd(d, p)^{113}Cd^a			
$E_{c.m.}$ (MeV)	$E_{c.m.}-6.799$ (MeV)	l	J^π	$\Gamma_{lj}{}^{(A)}$ (keV)	Γ(total) (keV)	S_{pp}	Excitation energy (MeV)	l	J^π	S_{dp}
9.674	2.875	3	$\frac{7}{2}^-$	0.62	29.0	0.02				
(9.717)	(2.918)	(3)	($\frac{7}{2}^-$)	0.70	70.0	(0.02)				
(9.796)	(2.997)	(2)	($\frac{5}{2}^+$)	0.20	25.0					
(9.850)	(3.051)	(0)	($\frac{1}{2}^+$)	1.70	35.0	(0.02)				
9.887	(3.088)	(2)	($\frac{5}{2}^+$)	1.20	60.0	(0.02)				
9.954	3.155	1	$\frac{3}{2}^-$	1.80	32.0	0.02				
10.062	3.263	1	$\frac{3}{2}^-$	1.60	55.0	0.02				
10.152	3.353	3	$\frac{7}{2}^-$	0.40	34.0	0.01				
(10.260)	(3.461)	(1)	($\frac{3}{2}^-$)	2.00	70.0	(0.02)				
(10.419)	(3.620)	(0)	($\frac{1}{2}^+$)	1.40	40.0	(0.01)				
10.513	3.714	1	$\frac{3}{2}^-$	1.80	32.0	0.02				

[a] L. H. Goldman *et al.*, Phys. Rev. **179**, 1172 (1969).

sums of the spectroscopic factors $\sum S_{pp}$ and $\sum S_{dp}$ for the single-particle states are tabulated in Table VI.

A. ^{110}Cd(p, p_0) and ^{110}Cd(d, p)

In general, there is a good one-to-one correspondence of states observed in the (p, p_0) and (d, p) measurements, although it is not clear why the $s_{1/2}(d, p)$ state at 1.19-MeV excitation was not seen in the (p, p_0) work. More levels are observed in the elastic-scattering work than were reported in the (d,p) measurements, and it is probable that the energy resolution (30 keV) prevented identification of these states in the (d, p) analyses. A comparison of spectroscopic factors for the two measurements is not possible since S_{dp} values are not reported.

B. ^{112}Cd(p, p_0) and ^{112}Cd(d, p)

For the $s_{1/2}$ ground state and for the $s_{1/2}$ states at excitation energies of 0.865 and 0.984 MeV, S_{pp} values are consistently larger than the corresponding S_{dp} values. Three $s_{1/2}$ levels at (d, p) excitation energies of 0.76, 1.90, and 2.08 MeV were not observed in the (p, p_0) work. The 1.90- and 2.08-MeV levels have very low S_{dp} values (0.02 and 0.01, respectively.) It is not

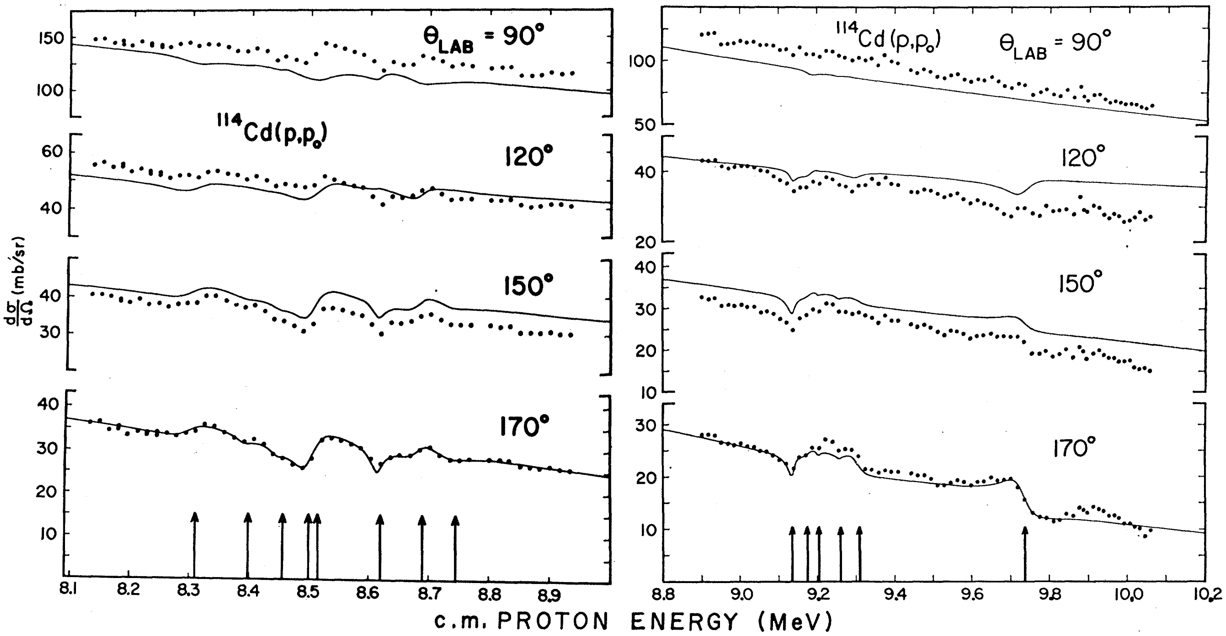

FIG. 9. Theoretical fits to the ^{114}Cd(p, p) elastic-scattering data at c.m. energies between 8.1 and 10.1 MeV. The arrows indicate the resonance energies as determined from the analysis.

TABLE V. Resonance parameters and spectroscopic factors determined from the theoretical fits to the ^{114}Cd(p, p) elastic-scattering data. A comparison of the ^{114}Cd(p, p) and ^{114}Cd(d, p) analyses is also shown.

^{114}Cd$(p, p_0)^{114}$Cd								^{114}Cd$(d, p)^{114}$Cd[a]		
$E_{\text{c.m.}}$ (MeV)	$E_{\text{c.m.}}-7.126$ (MeV)	l	J^π	$\Gamma_{lj}^{(A)}$ (keV)	Γ(total) (keV)	S_{pp}	Excitation energy (MeV)	l	J^π	S_{dp}
7.126	0.000	0	$\frac{1}{2}^+$	32.0	65.0	0.63	0.000	0	$\frac{1}{2}^+$	0.35
							0.178	5	$\frac{11}{2}^-$	0.33
7.363	0.237	2	$\frac{3}{2}^+$	9.80	45.0	0.49	0.227	2	$\frac{3}{2}^+$	0.53
7.491	0.365	2	$\frac{5}{2}^+$	1.70	32.0	0.09	0.357	2	$\frac{5}{2}^+$	0.096
							0.389	4	$\frac{7}{2}^+$	0.27
7.593	0.467	2	$\frac{3}{2}^+$				0.469	2	$\frac{3}{2}^+$	0.184
							0.503	2	$\frac{3}{2}^+$	0.103
(7.742)	(0.616)	(2)	$(\frac{5}{2}^+)$	0.42	19.5	(0.02)				
7.774	0.648	0	$\frac{1}{2}^+$	10.0	55.0	0.16	0.644	0	$\frac{1}{2}^+$	0.085
							0.695	(3)	$(\frac{7}{2}^-)$	0.0023
7.870	0.744	2	$\frac{3}{2}^+$	0.62	30.0	0.02	0.743	2	$\frac{3}{2}^+$	0.049
7.915	0.789	2	$\frac{3}{2}^+$	1.40	23.0	0.05	0.770	2	$\frac{3}{2}^+$	0.126
(7.951)	(0.825)	(0)	$(\frac{1}{2}^+)$	4.20	85.0	(0.06)	0.803	0	$\frac{1}{2}^+$	0.0061
							0.872	3	$\frac{7}{2}^-$	0.004
							0.896			
8.068	0.942	0	$\frac{1}{2}^+$	2.40	50.0	0.04	0.955	0	$\frac{1}{2}^+$	0.014
							1.042	(1)	$(\frac{3}{2}^-)$	0.0018
							1.062	4	$\frac{7}{2}^+$	0.045
8.196	1.070	2	$\frac{5}{2}^+$				1.085	2	$\frac{5}{2}^+$	0.024
							1.125			
(8.313)	(1.187)	(0)	$(\frac{1}{2}^+)$	4.60	70.0	(0.06)	1.175	0	$\frac{1}{2}^+$	0.021
							1.214	3	$\frac{7}{2}^-$	0.024
							1.248	2	$(\frac{5}{2}^+)$	0.012
							1.265			
(8.398)	(1.272)	(2)	$(\frac{5}{2}^+)$	0.26	28.0	(0.01)	1.308	2	$(\frac{5}{2}^+)$	0.011
(8.454)	(1.328)	(2)	$(\frac{5}{2}^+)$	0.30	25.0	(0.01)	1.326	2	$(\frac{5}{2}^+)$	0.022
							1.348	(4)	$(\frac{7}{2}^+)$	0.029
8.501	1.375	2	$(\frac{5}{2}^+)$	2.00	50.0	(0.07)	1.365	2	$(\frac{5}{2}^+)$	0.047
(8.515)	(1.389)	0	$\frac{1}{2}^+$	7.40	58.0	0.10				
							1.479			
(8.619)	(1.493)	(2)	$(\frac{5}{2}^+)$	1.20	26.0	(0.04)				
(8.688)	(1.562)	(0)	$(\frac{1}{2}^+)$	3.40	44.0	(0.04)	1.574			
							1.597	2	$(\frac{5}{2}^+)$	0.005
(8.744)	(1.618)	(2)	$(\frac{5}{2}^+)$	1.00	65.0	(0.03)	1.620	(2, 0)	$(\frac{5}{2}^+, \frac{1}{2}^+)$	0.0092
							1.725			
							1.818	2	$(\frac{5}{2}^+)$	0.0071
							1.840	(2, 0)	$(\frac{5}{2}^+, \frac{1}{2}^+)$	0.004
							1.876	(2)	$(\frac{5}{2}^+)$	0.013
							1.906	(2, 4)	$(\frac{5}{2}^+, \frac{7}{2}^+)$	0.021
9.036	1.910	1	$\frac{3}{2}^-$	1.50	22.0	0.02	1.928	(1)	$(\frac{3}{2}^-)$	0.016
(9.082)	(1.956)	(0)	$(\frac{1}{2}^+)$	1.90	40.0	(0.02)	1.954			
							1.976	(2, 4)	$(\frac{5}{2}^+, \frac{7}{2}^+)$	0.079
(9.104)	(1.978)	(1)	$(\frac{3}{2}^-)$	0.20	15.0		1.999	1	$\frac{3}{2}^-$	0.032
							2.019	1	$\frac{3}{2}^-$	0.013
(9.154)	(2.028)	(0)	$(\frac{1}{2}^+)$	0.16	20.0					
9.201	2.075	3	$\frac{7}{2}^-$	1.20	60.0	0.04	2.112			
9.624	2.498	3	$\frac{7}{2}^-$	3.80	75.0	0.12				

---

[a] J. B. Moorhead *et al.*, Phys. Rev. **165**, 1287 (1967).

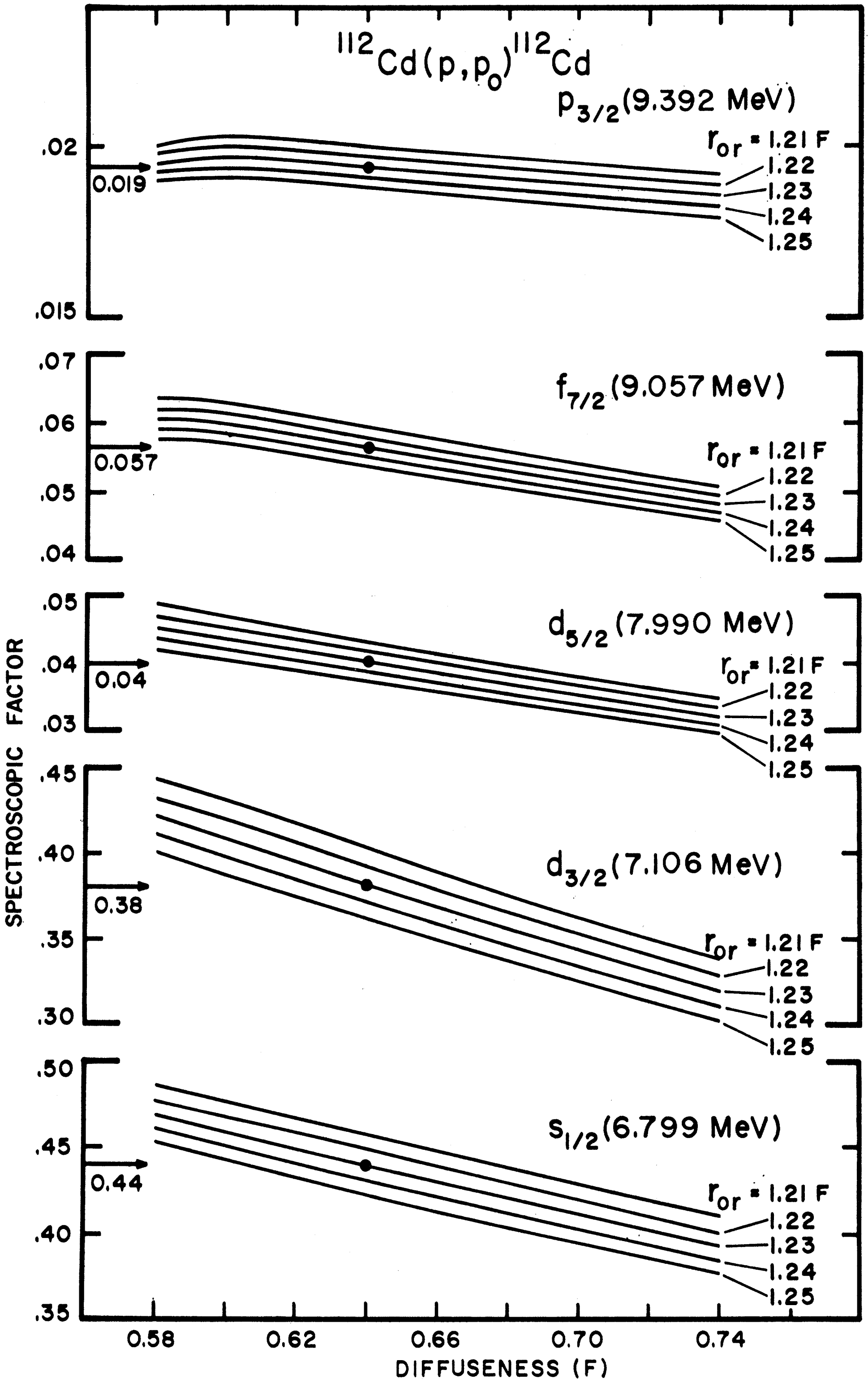

FIG. 10. A plot of spectroscopic factor as a function of real radius (r_{0r}) and diffuseness for the ^{112}Cd(p, p_0) analyses.

TABLE VI. A comparison of the sums of the spectroscopic factors ΣS_{pp} and ΣS_{dp} for the single-particle states, indicated as obtained in the respective (p, p) and (d, p) analyses.

l_j	^{111}In $\sum S_{pp}$	^{113}In $\sum S_{pp}$	^{113}Cd $\sum S_{dp}$	^{115}In $\sum S_{pp}$	^{115}Cd $\sum S_{dp}$
$s_{1/2}$	0.72	0.71	0.69	1.12	0.55
$d_{3/2}$	0.57	0.63	1.02	0.57	1.00
$d_{5/2}$	0.34	0.08	0.24	0.27	0.28
$f_{7/2}$	0.11	0.14	0.11	0.16	0.03
$p_{3/2}$	0.01	0.10	0.14	0.02	0.06

clear why the analog of the 0.76-MeV state was not seen. The parent analogs of $s_{1/2}$ levels at 2.160- and 2.213-MeV (p, p) excitation energies have l-value assignments of 1 in the (d, p) work.

Three $d_{3/2}$ levels at 0.90, 1.43, and 1.67 MeV, respectively, reported in the (d, p) work, were not observed in the elastic-scattering measurements. In general, however, S_{pp} values for $d_{3/2}$ analog resonances are in reasonable agreement with the corresponding S_{dp} values. The disagreement in the sums of the spectroscopic factors for $d_{3/2}$ states $\sum S_{dp}$ and $\sum S_{pp}$ is partly explained by the observation of more $d_{3/2}$ states in the (d, p) work than in the (p, p_0) measurements.

The rather strong $d_{5/2}$ state at 0.32-MeV (d, p) excitation energy was not observed in the (p, p_0) work. This state, apparently was not resolved from another d level only 20 keV below it with a total width of 33.7 keV. Consequently, there is a rather large discrepancy in the sums of the spectroscopic factors S_{dp} and S_{pp} for $d_{5/2}$ states.

The $f_{7/2}$ resonances observed in the (p, p_0) work are all above 9-MeV proton energy. The low-lying $f_{7/2}$ states observed in the (d, p) work at 1.58-, 2.04-, and 2.11-MeV excitation were not observed in the (p, p_0) data, probably because of penetrability considerations. However, the (d, p) l-value assignments for these very weak states are questionable. The parent states of the $f_{7/2}$ analog resonances at 2.258- and 2.635-MeV excitation energies are observed in the (d, p) work, but no spin assignments are given. The parent of the $f_{7/2}$ analog resonance at 9.555 MeV was assigned an l value of 1.

The analogs of the weak $p_{3/2}$ states at 2.17- and 2.31-MeV excitation in the (d, p) work were not observed. The parent analogs of the $p_{3/2}$ analog resonances reported above 2.87-MeV excitation energy in the elastic-scattering work were not reported. However, a comparison of the $p_{3/2}$ states observed in the two measurements is difficult because the $p_{3/2}$ states appear at high excitation and the $p_{3/2}$ single-particle strength is highly fractionized.

C. ^{114}Cd(p, p_0) and ^{114}Cd(d, p)

The parent analogs of the observed $s_{1/2}$ states at 1.562- and 1.956-MeV (p, p) excitation energies are reported in the (d, p) work, but spin assignments are not given. The sum of spectroscopic factors $\sum S_{pp}$ for $s_{1/2}$ states is 1.12, whereas the corresponding figure for $\sum S_{dp}$ is only 0.55, indicative of the discrepancy between S_{pp} and S_{dp} values for $l=0$ states. Except for the excellent agreement between the S_{pp} and S_{dp} values for the $d_{3/2}$ level at 7.363-MeV proton energy, the S_{dp} values are, in general, larger than S_{pp} spectroscopic factors for $d_{3/2}$ states. A good fit could not be obtained to the elastic-scattering data in the region of 7.6-MeV proton energy. Possibly, the analogs of the two closely spaced $d_{3/2}$ states at (d, p) excitations of 0.469 and 0.503 MeV had rather large total widths and could not be resolved by the single-level formula due to interference effects. The parent states of the $d_{5/2}$ analog resonances at excitation energies of 0.616 and 1.493 MeV are not reported in the ^{114}Cd(d, p) work. The analogs of the $d_{5/2}$ parent analog states at 1.248-, 1.597-, 1.818-, 1.840-, 1.876-, and 1.906-MeV excitation energies were not seen in the elastic-scattering data. All of these states have rather low spectroscopic factors and, in some cases, questionable spin assignments. In general, however, most of the $d_{5/2}$ analog resonances have spectroscopic factors in reasonable agreement with corresponding S_{dp} values.

The five weak levels (0.896, 1.125, 1.265, 1.479, and 1.725 MeV) reported in the (d, p) work with no spin assignments are not observed in the (p, p_0) measurements. It is probable that these states either have very low spectroscopic factors or correspond to high orbital-angular-momentum transfer values. As in the case of ^{112}Cd, a comparison of the $f_{7/2}$ states seen in the two measurements is difficult. The three $f_{7/2}$ states indicated in the (d, p) data lie below 1.3-MeV excitation, while

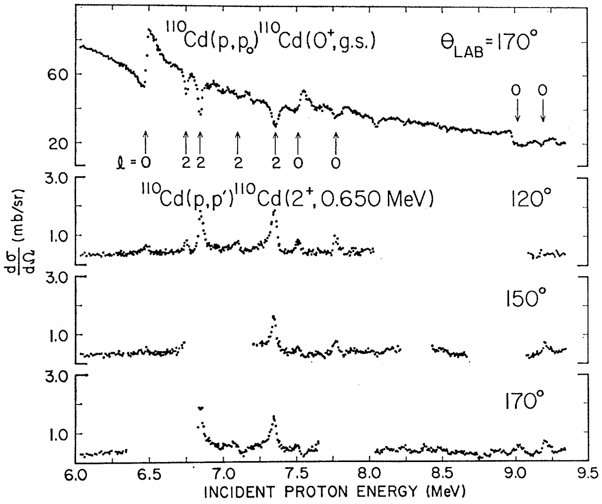

FIG. 11. ^{110}Cd$(p, p_0)^{110}$Cd and ^{110}Cd$(p, p_1)^{110}$Cd excitation curves. The yield to the 2^+ first excited state of ^{110}Cd is given. The location and respective l-value assignments of some of the more prominent of the elastic-scattering analog resonances are indicated in the figure.

the two observed f-wave analog resonances appear at excitations above 2 MeV. Two $p_{3/2}$ levels were observed in the (p, p_0) work, compared with four in the (d, p) analyses. However, the tentative $p_{3/2}$ state at an excitation of 1.042 MeV in the (d, p) work has an extremely small spectroscopic factor.

^{111}Cd, ^{113}Cd, and ^{115}Cd have 63, 65, and 67 neutrons, respectively, and it is to be expected that the sums of the spectroscopic factors for $d_{5/2}$, $d_{3/2}$, and $s_{1/2}$ single-particle states should generally decrease with the filling of the respective neutron subshells, that is, with the addition of neutrons. There is, however, very little evidence for such behavior. The sums of the spectroscopic factors $\sum S_{pp}$ for the three single-particle states remain remarkably constant for the three nuclei studied, with the exception of the low value of 0.08 for $\sum S_{pp}$ for $d_{5/2}$ states in ^{113}In. This discrepancy is apparently caused by the low resolution of the (p, p) work, as a result of which the analog of a strong (d, p) state at 0.32-MeV excitation was not resolved. However, it would appear that a state so strong should have been observed in the elastic-scattering work even if unresolved, so that the discrepancy must be considered rather puzzling. Although the sums of the spectroscopic factors for $s_{1/2}$ and $d_{3/2}$ states are approximately constant for the different nuclei in the (p, p) work, the lowest $s_{1/2}$ and $d_{3/2}$ states show a systematic increase in the spectroscopic factor with increasing mass number. Such effects could possibly be explained by the effects of the quadrupole-quadrupole force.

The dependence of the spectroscopic factor S_{pp} on the radius parameter r_{0r} and on the diffuseness a_r has been studied by evaluating the spectroscopic factor for a given radius for several different values of diffuseness. The results for ^{112}Cd(p, p_0) are shown in Fig. 10. As r_{0r} is varied, it is necessary, in order to maintain a good fit to the background elastic-scattering data, to vary a_r in such a way that the change in the spectroscopic factor is very small. That is, good fits to the elastic-scattering data can only be obtained for a certain range of r_{0r} and a_r, all of which predict approximately the same result for S_{pp}. The dot in each set of curves gives the real radius, and the real diffuseness for which a best fit to the experimental data was obtained.

The Coulomb displacement energy ΔE_C between the analog and the parent state is given by the relationship $\Delta E_C = E_p + Q_{dp} + E_d$, where E_p is the c.m. proton energy at which the analog resonance in the nucleus $(N, Z+1)$ occurs, Q_{dp} is the (d, p) reaction Q value, and E_d is the deuteron binding energy. The resulting Coulomb displacement energies for the analog pairs ^{111}Cd-^{111}In, ^{113}Cd-^{113}In, and ^{115}Cd-^{115}In are, respectively, 13.40, 13.34, and 13.27 MeV. These values are in good agreement with the respective values of 13.43, 13.34, and 13.26 MeV predicted by the empirical relationship of Long *et al.*[12]

$$\Delta E_C = -1.032 + 1.448 (Z/A^{1/3}),$$

where Z and A are the charge and mass numbers, respectively, of the parent analog nucleus.

The cross sections for inelastic proton scattering were generally low, as is expected since the analog resonances occur at rather low incident-proton energies and since the single-particle states in the parent nuclei are highly fractionated. The yield to the first excited (2^+) state in ^{110}Cd, $(E_x = 0.65$ MeV) is shown in Fig. 11. The 2_1^+ state resonates strongly at the pronounced low-lying $d_{5/2}$ and $d_{3/2}$ analog resonances and less strongly at the low-lying $s_{1/2}$ resonances. It is probable that the wave function of the core nucleus can be thought of as being built from not only the ground state but also from the first 2^+ excited state and that this second component contributes mainly to the inelastic-scattering resonances.

V. SUMMARY

Extensive measurements and analyses of proton elastic isobaric-analog resonances have been carried out using targets of ^{110}Cd, ^{112}Cd, and ^{114}Cd. A shell-model description of the analog resonances has been used in the analysis of the data. A comparison of the present work has been made with existing (d, p) work on the same targets, with good over-all agreement. Some of the low-lying analog resonances with high orbital-angular-momentum quantum numbers $l=4$ and 5 were not observed because of penetrability considerations. In addition, very weak (d, p) levels observed and analyzed in the high-resolution ^{114}Cd(d, p) and ^{112}Cd(d, p) measurements were not observed in the (p, p_0) work. Good over-all agreement was obtained between the deduced spectroscopic factors obtained in the two analyses. However, the spectroscopic factors S_{pp} for $l=0$ states were generally found to be larger than the corresponding S_{dp} values for the parent analog states. The spectroscopic factors deduced from the analysis of the proton-elastic-scattering data for the analog states have been shown to be rather insensitive to the choice of optical parameters. Within the experimental uncertainties, the experimentally found Coulomb displacement energies agree very well with the valus obtained using the empirical relationship of Long *et al.*[12]

ACKNOWLEDGMENTS

The authors wish to thank Miss V. Haravu and W. L. Lafuze for assistance in taking the data and Dr. S. A. A. Zaidi for helpful discussions concerning the analysis.

---

[12] D. D. Long, P. Richard, C. F. Moore, and J. D. Fox, Phys. Rev. **149**, 906 (1966).

PHYSICAL REVIEW C VOLUME 1, NUMBER 4 APRIL 1970

Cumulative Author Index

All authors published so far in the current volume are listed alphabetically with the issue and page numbers following the dash. A cumulative author and subject index covering Physical Review A *through* D *is published every six months under separate cover.*